CHALMERS
UNIVERSITY OF TECHNOLOGY

UNIVERSITY OF GOTHENBURG

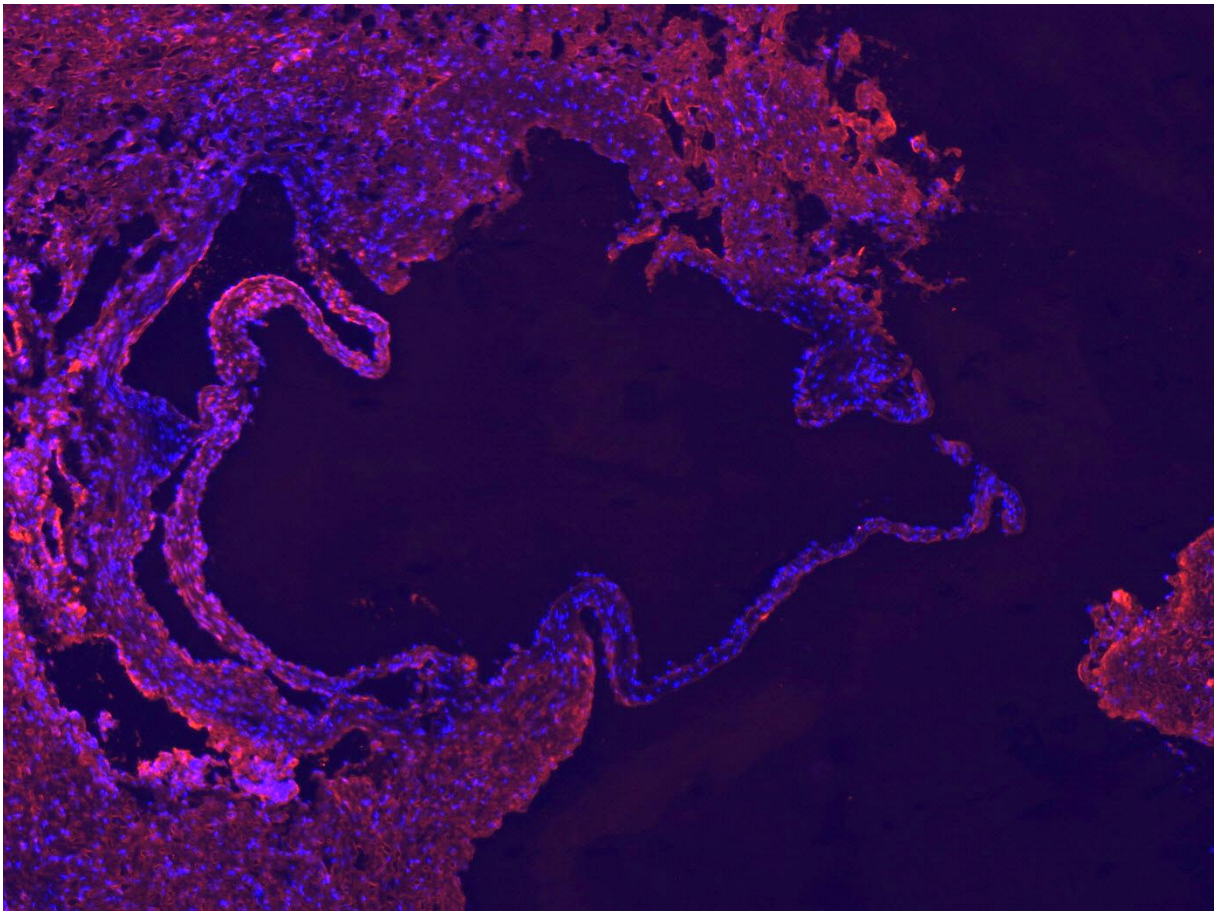

# STK25

## A new regulator of the risk of metabolic liver disease and cardiovascular disease risk

Master's thesis in Molecular Medicine

ELIN MAGNUSSON

Lundberg Laboratory for Diabetes Research
Department of Molecular and Clinical Medicine
UNIVERSITY OF GOTHENBURG

CHALMERS UNIVERSITY OF TECHNOLOGY
Gothenburg, Sweden 2018

**THESIS SUBMITTED**

**FOR THE PARTIAL FULFILLMENT**

**OF**

**MASTER OF SCIENCE in BIOTECHNOLOGY**

# STK25

## A new regulator of the risk of metabolic liver disease and cardiovascular disease risk

ELIN MAGNUSSON


CHALMERS
UNIVERSITY OF TECHNOLOGY

CHALMERS UNIVERSITY OF TECHNOLOGY
Gothenburg, Sweden 2018

STK25

A new regulator of the risk of metabolic liver disease and cardiovascular disease risk

Elin Magnusson



Supervisor: Dr Emmelie Cansby, Lundberg Laboratory for Diabetes Research, Department of Molecular and Clinical Medicine, Gothenburg University

Co-supervisor: Assoc. Prof Margit Mahlapuu, Lundberg Laboratory for Diabetes Research, Department of Molecular and Clinical Medicine, Gothenburg University

Examiner: Prof. Stefan Hohmann, Biology and Biological Engineering, Systems and Synthetic Biology, Chalmers University of Technology

Master's Thesis 2018:01
Chalmers University of Technology
SE-412 96 Gothenburg
Telephone +46 31 772 1000

Cover: Immunofluorescent detection of STK25 in aortic root section of *Stk25* transgenic mouse.

# Preface

This project was performed for the partial fulfilment of Master's in Science in Biotechnology, at the Lundberg Laboratory for Diabetes Research at the Department of Molecular and Clinical Medicine, Gothenburg University, Sweden. The project was initiated in September 2017 and finished in February 2018. The project was carried out under the supervision of Dr Emmelie Cansby, Gothenburg University and co-supervisor Assoc. Prof Margit Mahlapuu, Gothenburg University. Examiner was Prof. Stefan Hohmann, Chalmers University of Technology.

The project was founded by the Swedish Research Council, the Novo Nordisk Foundation, the Swedish Heart and Lung Foundation, the Diabetes Wellness Network Sweden, the Swedish Diabetes Foundation, the Royal Society of Arts and Sciences in Gothenburg, the Wiberg Foundation, Längmanska Kulturfonden, the Adlerbert Research Foundation, the I. Hultman Foundation, the S. and E. Goljes Foundation, the West Sweden ALF Program, the F. Neubergh Foundation, the I.-B. and A. Lundbergs Research Foundation, the Swedish Innovation Agency Vinnova, and the European Foundation for the Study of Diabetes and Novo Nordisk Partnership for Diabetes Research in Europe.

# Abstract

Cardiovascular diseases (CVDs) are today the leading cause of death, accounting for 31% of all deaths globally. Recently, attention has focused on the importance of non-alcoholic fatty liver disease (NAFLD) and non-alcoholic steatohepatitis (NASH) in the development and progression of CVDs.

Recent studies, by the research group of Assoc. Prof. Margit Mahlapuu, Gothenburg University, have identified serine/threonine kinase 25 (STK25), a protein belonging to the sterile 20 kinase superfamily, as a key regulator of liver lipid metabolism, whole-body glucose and insulin homeostasis, and the progression of NAFLD/NASH, based on results from well-characterized patient populations, cultured human cells and unique mouse models.

The aim of this project proposal is to elucidate the integrated molecular mechanisms linking NAFLD/NASH to CVD, with the focus on the novel mediator STK25. Importantly, the study has a potential to lay a scientific basis to reduce CVD risks and to find novel therapeutic strategies for its treatment.

The role of STK25 in the plaque progression of atherosclerosis was studied using *Stk25* transgenic (TG) and knockout (KO) mice with low-density lipoprotein receptor (LDLR) deficiency induced through a single injection of recombinant adeno-associated virus (rAAV) encoding gain-of-function mutant of proprotein convertase subtilisin/kexin type 9 (PCSK9), combined with an atherogenic western-type diet.

The plaque maturation and lesion area were evaluated by histological studies in aortic root sections together with measurements of NASH progression in liver samples. *Stk25* TG mice displayed an increase in lesion area, plaque maturation, inflammatory response as well as more advanced NASH, compared to their corresponding wildtype (WT) littermates. Reciprocally, *Stk25* KO mice demonstrated decreased plaque formation, aggravated lesions and less signs of NASH, compared to their corresponding WT littermates.

The results of this project provide evidence that STK25 plays an important part in the progression of atherosclerosis due to excess dietary intake. Further studies are needed to understand the upstream regulators, and the downstream targets, in the signalling pathway of STK25.

Key words: STK25, cardiovascular disease, CVDs, NAFLD, NASH, PCSK9, atherosclerosis

# Contents

# List of abbreviations

| | |
|---|---|
| **STK25** | Serine/threonine kinase 25 |
| **CVDs** | Cardiovascular diseases |
| **NAFLD** | Non-alcoholic fatty liver disease |
| **NASH** | Non-alcoholic steatohepatitis |
| **T2D** | Type 2 diabetes |
| **PCSK9** | Proprotein convertase subtilisin/kexin type 9 |
| **rAAV** | Recombinant adeno-associated virus |
| **LDL** | Low-density lipoprotein |
| **LDLR** | Low-density lipoprotein receptor |
| **SMC** | Smooth muscle cells |
| **KO** | Knockout |
| **TG** | Transgenic |
| **WT** | Wildtype |
| **OCT** | Optimal cutting temperature |
| **ORO** | Oil Red O |
| **DHE** | Dihydroethidium |
| **PBS** | Phosphate buffered saline solution |
| **PBS-T** | Phosphate buffered saline tween solution |
| **BSA** | Bovine Serum Albumin |
| **ROS** | Reactive oxygen species |
| **AST** | Aspartate aminotransferase |
| **DAPI** | 4′, 6-diamidino-2-phenylindole |

# 1 Introduction

With its steep increase in incidence, obesity is becoming one of the major global threats to human health. Approximately 650 million adults worldwide or 13% of the adult world population are characterized as obese and the number have nearly tripled since the 1970s [1]. Known consequences of obesity are several metabolic diseases, e.g. cardiovascular diseases (CVDs), type 2 diabetes (T2D) and liver diseases, such as non-alcoholic fatty liver disease (NAFLD) and non-alcoholic steatohepatitis (NASH) [2, 3].

The recent increase in obesity is linked to the worldwide adoption of a lifestyle with a high-fat and high-energy dense diet [1]. The average calorie intake around the world is around 2800 kcal per person and day, high over the recommended daily allowance [4] and the number is only thought to rise in the future, giving cause for concerns since the related conditions often are deadly.

CVDs, such as atherosclerosis and coronary heart disease, are at date the number one cause of death worldwide, with 31% of all deaths related to CVDs [5]. Treatments of CVDs are often costly and may require surgical interventions that may not solve the problem indefinitely [5], and other treatment options, and preventative strategies, are therefore of outmost importance.

A similar increase in liver disease related to obesity has also been established, with NAFLD being among the most common [6] with around one-third of the human population being affected worldwide [7].

Recent research has therefore focused on obesity and the related diseases to find possible treatments or prevention methods [2]. However, the understanding of the mechanisms of the pathophysiological link between obesity and related diseases remain unclear. The goal of identifying possible molecules that can be used as treatment targets are therefore of importance, but also the ability to treat more than one of the diseases at the same occasion.

The research group of Assoc. Prof. M. Mahlapuu has recently discovered the serine/threonine kinase 25 (STK25) as a new key regulator of metabolism and potential target for the treatment of metabolic disease [3, 8–11], although the effects of the kinase on CVDs are not known. Based on these studies, we therefore wanted to elucidate the role of STK25 in atherosclerosis, one of the most common CVDs today that causes a high number of deaths yearly, and as a possible mediator in the molecular network associating NAFLD/NASH and cardiovascular risks.

# 2 Aims and objectives

The goal of the work performed during this project was to evaluate the effects of STK25 on atherosclerosis, using a newly developed mouse model where injection of proprotein convertase subtilisin/kexin type 9 (PCSK9), in combination with feeding of a western-type diet, is used to induce atherosclerosis [12]. The PCSK9 mice model was used in combination with already established mouse models of *Stk25* overexpression and knockdown. The possible effects on plaque formation in the aorta and liver damage, were investigated and evaluated.

The objectives of the projects are the following:

- Investigate the role of STK25 in the development and aggravation of atherosclerosis
- Evaluate if STK25 inhibition enables to achieve regression/resolution of atherosclerosis
- Investigate if STK25 is a critical mediator and link between NAFLD/NASH and CVDs.

# 3 Background

The increasing adoption to a diet, high in fat and energy content, causes higher number of people to become overweight or obese [13], causing higher numbers of CVDs and liver diseases correspondingly.

The need for treatments and care for people affected by obesity and the related conditions causes high demands on the society but also on the healthcare system, both economically and resource consuming [4]. Since the prevalence is predicted to increase even more rapidly, it is therefore even more important to discover and develop new treatments to meet the increasing demand.

Obesity that is left untreated for too long will eventually give rise to metabolic disorders. If the condition is detected in the early stages of the development, then a lifestyle change can be sufficient to reverse or slow down the progression, such as decrease in calorie intake, diet change and increased energy expenditure [14]. If the metabolic diseases are at an advanced level, they can be hard to treat, with the different conditions often having to be treated separately and for long periods of time [15]. In many cases the treatments will be lifelong. Surgical interventions might also be needed if the diseases become too critical or advanced to treat with regular methods.

## 3.1 Cardiovascular disease and atherosclerosis

CVDs are the leading cause of death globally and the number of people suffering from it are steadily on the rise [5, 16]. The risk of developing CVDs, such as hypertension, coronary heart disease and heart failure, increases greatly for patient suffering from obesity [13]. The primary cause of heart disease and stroke is atherosclerosis, where a formation of plaques in the arteries disrupts or stops the blood flow [17]. The laminar flow in the tubular regions of the arteries provides low shear stress on the epithelial cells covering the inside wall of the blood vessels, but arterial branching or curvature changes the blood flow, causing higher stress on the cell layer. The higher stress from the turbulent flow causes the cell layer to have a higher permeability for macromolecules such as lipids, making it a preferential site for the formation of plaques [17, 18]. The accumulation of lipids can progress into a fatty streak, where the level of low-density lipoprotein (LDL) increases and promotes swelling and inflammation of the area, causing macrophages to be recruited to the site [17].

Highly oxidized LDL is taken up by macrophages to start the formation of foam cells. The cholesterol-carrying macrophages accumulates in the subendothelial layer of the arterial wall and further promotes inflammation and swelling of the lesion area. The advancement of the lesions can progress to a fibrous lesion that contains a lipid-rich necrotic core with a fibrous content, consisting of smooth muscle cells (SMC) and SMC-derived extracellular matrix [17]. Severely advanced plaques can rupture and cause further damages such as stroke or myocardial infarction by blocking vital blood vessels [19].

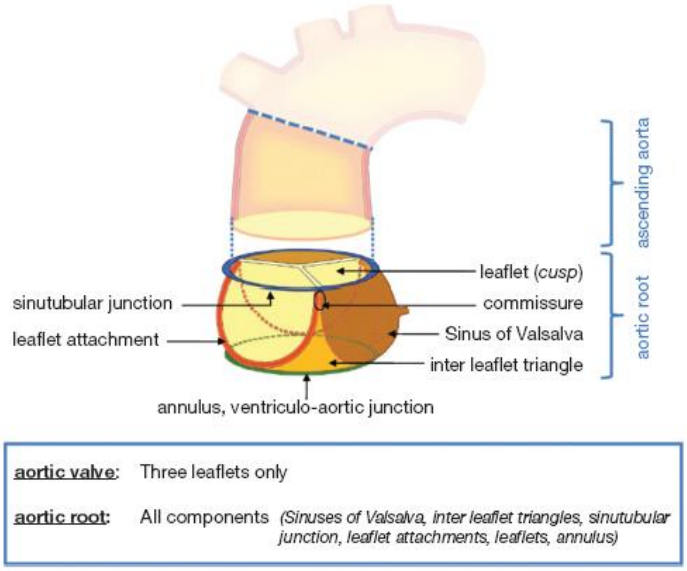


**Figure 1: Illustration of the anatomy of the aortic root as described by [18].**

Common sites for plaque formation are in the abdominal aorta, coronary arteries and carotid arteries [18] since the flow pattern often are affected with a more turbulent flow. The ability to study atherosclerosis have led researchers to study the aortic root (Figure 1), a site prone to quickly develop plaques due to the placement, the shape and the large volumes of fluids through it [12]. Located at the beginning of the aorta, the aortic root connects the circulation system to the heart [20] and the main function of the root is to control the blood flow out from the left ventricle.

## 3.2 NAFLD and NASH

During recent years, an increase in liver diseases have been noticed worldwide. People with obesity are at a high risk of developing NAFLD [8]. The definition of NAFLD is the presence of macrovesiclar steatosis in more than 5% of the hepatocytes in a patient that consume little to no alcohol [21].

The prevalence of NAFLD is steadily on the rise globally and it is now the leading chronic liver disease in the Western world, with around one third of the adult American population suffering from NAFLD [7, 21]. A similar rise in the prevalence of NAFLD can be seen in Asian countries such as China and Japan, with 15-30% and 20-30% respectively [21].

The disease includes a broad variety of symptoms, ranging from simple steatosis to more severe degrees of hepatocyte inflammation or necrosis and liver fibrosis [6, 7]. Approximately 10%-20% of patients suffering from NAFLD will progress to NASH, a state that includes features such as liver inflammation, fibrosis, fatty infiltration and hepatocyte damage [8]. The risk of developing cirrhosis, hepatocellular carcinoma and liver failure increases greatly for patients suffering from NASH [8]. To date there are no drugs approved for treatment of NASH, often making liver transplant the only option for patients suffering from severe NASH [22, 23]. A reliable non-invasive therapeutic treatment is therefore needed.

## 3.3 STK25

The sterile 20 (STE20) kinase superfamily contains several different described members and can be divided into two families; the germinal centre kinase (GCK) family with the kinase domain located at the N-terminal and the p21-activated protein kinase (PAK) family with a C-terminal located kinase domain [10, 24].

STK25, also known as YSK1 or SOK1, from the GCKIII subfamily, was first described in 1996 as a 426 long amino acid kinase [24]. The kinase have been located to the Golgi apparatus, where it is an active part in the localization and morphology of the complex [10]. STK25 has also been shown to be slightly activated by oxidative stress inducers but not by other environmental stresses, such as osmolar stress or heat shock [10]. Further studies of the STK25 have also shown that the kinase are involved in the regulation of cell migration and cell death [10].

Recent studies by the research group of Assoc. Prof. M. Mahlapuu have identified STK25 as a possible target for treatment of lifestyle-related metabolic disorders, such as T2D, NAFLD and NASH. It was found that the high-fat fed TG mice display impaired whole-body glucose and insulin homeostasis and an increase in liver triglyceride accumulation, lipid droplet size and density, as well as increased liver fibrosis and hepatocellular damage [8, 9]. Reciprocally, high-fat diet fed *Stk25* KO mice showed suppression of the development of hyperinsulinemia and hyperglycemia together with increased insulin sensitivity [9]. A reduction in liver lipid accumulation, inflammation and fibrosis was also seen in *Stk25* KO mice compared to WT littermates [3]. STK25 was furthermore discovered to be localized on the surface of hepatic lipid droplets, effecting β-oxidation, triacylglycerol secretion and lipid uptake [8].

To further investigate the role of STK25 in the progression from NAFLD to NASH, the expression of STK25 in relation to NASH in human liver biopsy material was evaluated [3, 25]. A significant correlation could be found in the *Stk25* mRNA expression and the signs of NASH, such as liver steatosis, inflammation and ballooning. Furthermore, STK25 protein levels correlate significantly and positively with NASH development in human liver biopsies, supporting a critical role of STK25 in the pathogenesis of NAFLD in humans.

## 3.4 PCSK9 and rAAV

High levels of LDL in the blood plasma is a risk factor that has been linked to the development of CVDs, such as atherosclerosis [17]. The LDL receptor (LDLR), located in the membrane of the hepatocytes, mediates the uptake of LDL from the circulation and transports it into the hepatocytes in a clathrin-coated capsule for lysosomal degradation. The receptor is then recycled and transported back to the membrane of the hepatocytes [26]. Genetic defects in the LDLR in humans are associated with several hyperlipidemic disorders, including familial hypercholesterolemia, that are known to increase the susceptibility to developing atherosclerosis [27, 28].

The need to study plaque formation and the molecular interactions involved in the process requires good animal models. Recently *Bjørklund et. al* [12] developed an alternative method to induce atherosclerosis in mice, circumventing the time consuming breeding process often needed for other models like LDLR deficient mice. The method combines the use of a single injection of proprotein convertase subtilisin/kexin type 9 (PCSK9) and

recombinant-adeno-associated virus (rAAV) encoding gain-of-function of PCSK9. PCSK9 binds LDLR, directing it for lysosomal degradation, thus increasing the LDL levels in the blood, which subsequently increases plaque formation [12, 17]. AAV is a single-stranded DNA virus with a small protein capsule, belonging to the family of parvoviridae, that only produces a mild immune response [29]. The virus is unable to replicate without the help of a helpervirus, such as adenovirus or herpesvirus. Inside the cells, the rAAV vector is present in concatemeric episomal forms and therefore further reducing the risk of mutagenesis due to insertions [29]. To test if the viral vector causes any immune response, the levels of aspartate aminotransferase (AST) are measured in blood samples. AST is released from damaged hepatocytes as a response of the induction of T cells [30], and increased activity is therefore an indirect sign of liver damage.

LDLR is expressed in several tissues, such as the liver, small intestine and the colon [31]. Different viral vectors are available depending on the desired target, with serotype 7, 8 and 9 being hepatocyte-specific [32], making them a good option to use when targeting the liver.

## 3.5 C57Bl/6J and C57Bl/6N mice

The ability to study different human diseases in animal models have led to the development of mice with specific characteristics, such as the C57Bl/6 strain. C57Bl/6J mice are often used for transgenic studies since the strain has a high susceptibility to induced mutations and the strain also has a high ability to develop diet-induced obesity, NAFLD/NASH and atherosclerosis [33]. The C57Bl/6N strain also has the susceptibility to develop metabolic diseases when given a high-fat diet, although not as fast as C57Bl/6J [34].

## 3.6 Histological studies and staining techniques

Histology is the use of microscopic techniques to study cells and tissues after preparation, sectioning and staining [35]. The process enables samples to be analysed by microscopy.

### 3.6.1 Cryosectioning of frozen samples

The process of degradation of a sample from a living being starts immediately after removal from the host and the sample will therefore have to be either analysed and studied *in situ* or the sample will have to be preserved for later assessment. One common procedure is to freeze samples and to store them for future analysis since the freezing process temporarily stops the degradation but also allows the sample to uphold its structure.

Cryosectiong is a method that allows cross-sectional studies to be carried out on frozen samples [36, 37]. The method is often used as a preparation technique for histological studies, since it has the ability to make thin sections of a sample without disrupting the structure. The sample is placed in an embedding medium that will preserve and hold the samples during the freezing and the procedure. Common embedding mediums to use are agars and glycerine based mediums [38]. The frozen sample are mounted in a microtome cryostat and then sectioned at a desired thickness, often μm thick. The sections are collected on microscope glass slides and the embedding medium is allowed to melt and evaporate before freeze storing or histological evaluation of the sections [37, 39]

## 3.7 Immunohistochemistry and immunofluorescence

The detection of specific targets can be achieved by using immunofluorescence, a form of immunohistochemistry. The technique utilizes the presence of specific antigens expressed on the desired target. A primary antibody binds to the desired antigen, if present, in a sample. A fluorophore-labelled secondary antibody that is specific for the primary antibody is then applied. If any cells in a sample express the targeted antigen it can be detected by exposing the sample to the corresponding wavelength of the probe [40].

# 4 Methods and materials

## 4.1 Mouse model – hPCSK9-injected mice

*Stk25* TG mice were generated and genotyped as described by *Cansby, E. et. al*. [11]. *Stk25* KO mice were generated and genotyped accordingly as described by *Matsuki, T. et. al*. [41]. In this study, *Stk25* TG and KO mice were compared with their corresponding wild-type (WT) littermates since the genetic background of these lines differs (C57BL6/N for *Stk25* TG mice and C57BL6/J for *Stk25* KO mice). All mice were kept 3 to 5 animals in each cage in a temperature controlled room (21°C) with a 12-hour light-dark cycle. All animals had free access to food and water.

Male KO mice (called KO/hPCSK9 in this report) and their WT littermates and male TG mice (called TG/hPCSK9 in this report) with their corresponding WT littermates were injected at 8 weeks of age with a single tail vein injection of rAAV ($2x10^{11}$ vector genome copies) with mutant PCSK9 (human) serotype 8 (rAAV8-D374Y-hPCSK9). A control group of WT littermates (called WT/saline in this report) was injected with saline solution for both cohorts (Figure 2).

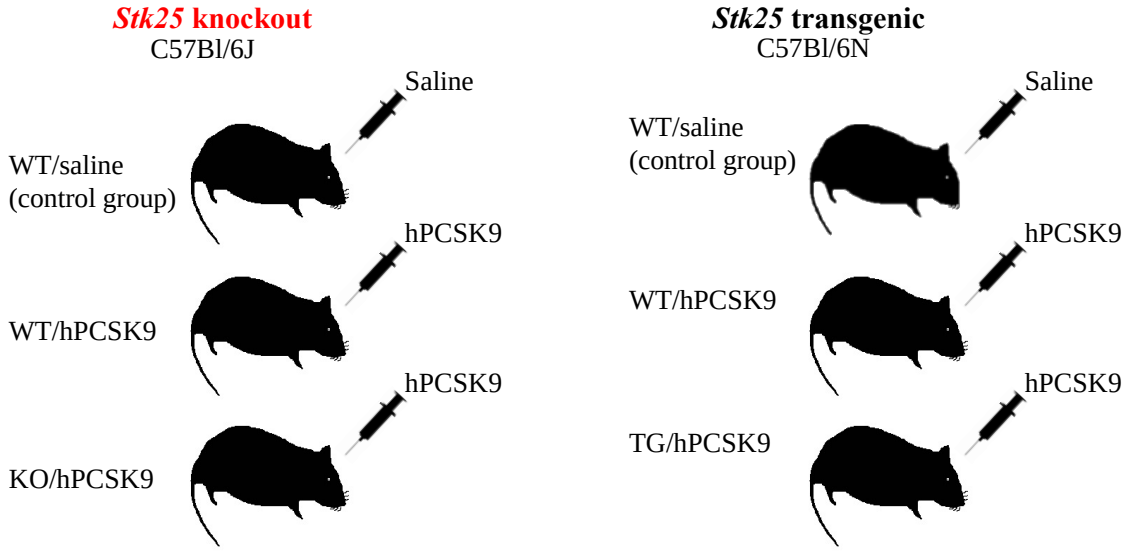


**Figure 2: Schematic overview describing the two mice cohorts used during the project and their corresponding injection treatment.**

The cohort was then challenged for 12 weeks with a western-type diet (21% fat, 0,2% cholesterol). The mice were killed at 20 weeks of age after 4 hours of fasting. Blood samples were collected by heart puncture with a syringe. Liver samples were collected and fixed in paraffin or snap frozen in liquid nitrogen and stored at -80°C. The aorta and aortic root were removed and divided through careful incision. The aortic root was placed in optimum cutting temperature (OCT) medium in a small cryomold and snap frozen in liquid nitrogen. Samples were then stored at -80°C for further analysis.

Before the start of the experiments, conformation of PCKS9 treatment was done by qRT-PCR and Western blot analysis, as previously described [11]. This work was done by supervisor Dr Emmelie Cansby.

## 4.2 Cryosectioning of the aortic root

The frozen aortic root sample was removed from the cryomold and fixed to a chuck with a small amount of OCT. The chuck was then placed in the cryostat to allow rapid freezing of the OCT medium. The cryostat was kept between -25°C and -20°C to avoid any damages of the sample.

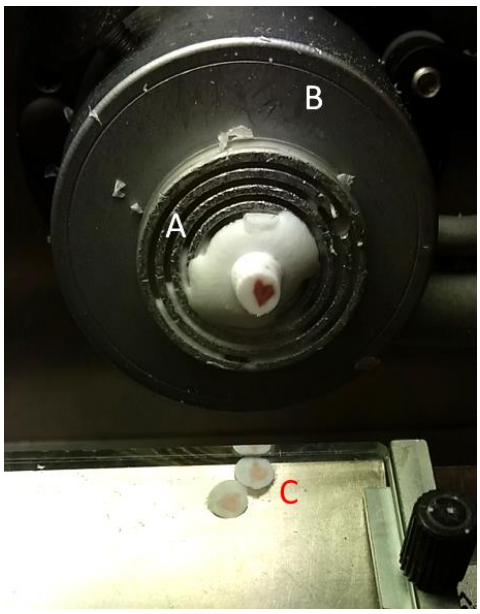


**Figure 3: Illustrative picture of aortic root sample mounted in cryostat. A) Mounted aortic root on chuck B) Arm C) Sliced sections of sample**

The chuck was then locked into the arm and positioned accordingly. All excess sample and medium was then removed to reach the aortic root (Figure 3). At the starting point of the aortic root, the section thickness was set to 8 µm and four consecutive sections were picked on a glass slide. The fifth section was then discarded to receive an even length of sample of 40 µm on each slide. All glass slides were then kept at -20°C until further use.

## 4.3 Hydroxyproline

One method that are used in research studies to study liver damages, are to measure hydroxyproline content in liver samples as a marker for fibrosis [42]. Hydroxyproline is an amino acid component in collagen, a protein that is the major component in fibrosis [43] and elevated levels can be found in liver samples with developed NASH.

The hydroxyproline content in liver samples was measured by using the Hydroxyproline Assay Kit from Sigma-Aldrich (Cat. No: MAK008).

Around 40 mg of liver sample was homogenized in a 10-fold equivalent volume of MilliQ water using a QIAGEN TissueLyser II for 2.5 minutes at 2500 Hz.
100 µl of each sample was then transferred to a 2 ml micro tube containing 100 µl HCl (12 M) and incubated for 3 h at 120°C.

30 µl of each sample was then transferred to a 96-well plate and incubated to dryness at 60 °C. The standard solution was added to the plate in the concentrations of 0, 0.2, 0.4, 0.6, 0.8, 1.0 µg/well. All samples and standards were run in duplicates.

Chloramine T/Oxidation Buffer Mixture was mixed by adding 6 µl Chloramine T Concentrate to 94 µl Oxidation Buffer and 100 µl was added to all wells and incubated at room temperature for 5 minutes. The Diluted DMAB Reagent was mixed by adding 50 µl of DMAB Concentrate to 50 µl Perchloric Acid/Isopropanol Solution and 100 µl was then added to each well and incubated at 60°C for 90 minutes.

The absorbance was measured at 560 nm by using a Tecan Infinite M200 Pro Microplate Reader. The concentrations of hydroxyproline for each sample was calculated by using the equation generated by the standard curve and divided by the sample volume.

## 4.4 AST assay

The AST activity in blood plasma samples were analysed using Aspartate Aminotransferase Activity Assay Kit (Cat. No: MAK055) from Sigma-Aldrich accordingly to provided protocol. 10 µl of plasma sample was added to a well on a 96-well plate and brought to a final volume of 50 µl by adding 40 µl of AST Assay Buffer. All samples and standards were run in duplicates.

The Glutamate Standard was loaded onto the plate and brought to a final volume of 50 µl by addition of AST Assay Buffer. The used standard concentrations were 0, 1, 2, 4, 6, 8, and 10 nmole/well.

5 µl of AST Positive Control was added to a well and brought to a final volume of 50 µl by addition of 45 µl AST Assay Buffer.

The Master Reaction Mix was prepared by mixing AST Assay Buffer, AST Enzyme Mix, AST Developer and AST Substrate together (8:2:8:1).

100 µl Master Reaction Mix was then added to each well and mixed by using a horizontal shaker to start the reaction. The plate was then incubated in the dark at 37°C and the absorbance was measured at 450 nm every 5 minutes during 1 hour by using a Tecan Infinite M200 Pro Microplate Reader. The change in activity ($\Delta B_{Final-Initial}$) was calculated by using the change in absorbance between two time points, compared to the generated standard curve. The final AST activity was calculated by Equation 1.

$$AST\ activity = \frac{\Delta B_{Final-Initial} \times Dilution\ factor}{(Reaction\ time) \times V_{sample}} \quad (1)$$

## 4.5 Histological studies

### 4.5.1 Staining procedures

#### *4.5.1.1 Oil Red O*

Oil Red O (ORO) is a stain used for histological studies of lipids in frozen tissue sections, were the lipids will be seen as red against the background. The method can be used to visualize the morphology and localisation of lipids and lipid droplets. The stain is fat-soluble and stains neutral lipids and cholesteryl esters, making the dye very specific since it does not bind and stain biological membranes [44].

Glass slides with aortic root section from three different levels (0, 80 and 160 μm) were thawed at room temperature and placed in a 24-slide rack. All steps were carried out at room temperature.

All sections were fixed in 4% vol./vol. phosphate-buffered formaldehyde for 20 minutes before being immersed in isopropanol (60%) for 1 minute. The slides were then placed in Oil Red O solution for 15 minutes and quickly submerged in isopropanol. All slides were then washed in deionized water and placed in Mayer HTX (Hematoxylin solution) for 1 minute before being rinsed with running water for 15 minutes until the water was clear of blue colour. The slides were then carefully dried and mounted with glycerol (30%) and covered with a glass cover slide. Photos of the sections were taken with Apotome Axioplan 2 Imaging Microscope at 20x magnification.

#### *4.5.1.2 Picrosirius Red*

The Picrosirius Red stain is used to visualize collagen fibers in tissue samples. Stained collagen fibers will appear as red, clearly distinguishing the fibers from the surrounding tissue [45]. Picrosirius are widely used during histological studies since the presence of higher amounts of stained collagen fibers are a sign of fibrosis in a tissue sample [46]. The stain is specific for collagen type I and type III [47]. The fibrosis detected in NAFLD and NASH have increased levels of collagen type I present [48], but a higher collagen content is also a sign of plaque advancement in atherosclerosis [17].

Glass slides with frozen sections of aortic roots from one level were thawed at room temperature. The slides were then placed in a 24-slide rack and fixed with 4% vol./vol. phosphate-buffered formaldehyde for 20 minutes. All steps were carried out in room temperature if no other temperature is specified. The slides were then washed (3x2 minutes) in water. The slides were then transferred to preheated Bouin's solution and fixed for 45 minutes in 50°C. The slides were then washed again (3x2 minutes) in water and immersed in 1% acidic acid for 2 minutes. All slides were then washed (3x2 minutes) in water before immersion in Picrosirius Red (2%) for 30 minutes. Washing with water (3x2 minutes) was then done before the slides were removed from the rack and carefully air-dried. The sections were then mounted with 30% glycerol and covered with a glass slide. Photos of the sections were then taken in Apotome Axioplan 2 Imaging Microscope at 20x magnification.

### 4.5.2 Immunofluorescence

#### *4.5.2.1 STK25 and DAPI*

The localization and presence of STK25 in tissue sections can be visualized by using immunofluorescence. The primary antibodies are designed to bind to antigens specific for STK25 and have the ability to bind secondary fluorophore-carrying antibodies for detection. The correct binding of the antibody complex will be seen as a fluorescent signal when submitted to the correct wavelength during optical microscopy.

4′, 6-diamidino-2-phenylindole (DAPI) is a fluorescent probe that can be used for staining of cell nuclei. The dye has a high cell membrane permeability and forms a strong fluorescent

probe-DNA complex by binding to the minor groove of AT-rich sequences of the DNA [50, 51]. The binding of the complex will enhance the fluorescent from the probe.

Glass slides with frozen sections of aortic roots from one level were thawed at room temperature and placed in a 24-slide rack. All steps were carried out at room temperature.

The sections were fixed in 4% vol./vol. phosphate-buffered formaldehyde for 20 minutes before washing with phosphate buffered saline solution (PBS) (2x2 minutes). All sections were then blocked with 5% goat serum in PBS containing 1% bovine serum albumin (BSA) for 1 hour before washing with PBS (2x2 minutes). The primary antibody (STK25) was diluted in PBS (1:750) and applied to all slides and incubated in the dark for 1 hour before washing (PBS 2x2 minutes). The secondary antibody (Alexa 594) was diluted in PBS (1:1000), applied to all slides and incubated in the dark for 1 hour before washing (PBS 2x2minutes). DAPI solution (300nM) were applied to all sections and incubated for 3 minutes under cover. All slides were washed with PBS (2x2 minutes) and air-dried before mounting with ProLong Gold Antifade Reagent and covered with a glass cover. Photos of the sections were then taken in Apotome Axioplan 2 Imaging Microscope at 20x magnification

#### *4.5.2.2 DHE*

Oxidative stress is a sign of cellular dysfunction and damage. The development of plaques during atherosclerosis causes the involved epithelial cells to release higher levels of reactive oxygen species (ROS) [17, 49]. The level of ROS can be detected by using Dihydroethidium (DHE). The dye will be oxidized in the presence of superoxide, forming a red fluorescent product that can be detected.

Glass slides with frozen sections of aortic roots from one level were thawed. All steps were carried out at room temperature. The slides were then placed in a 24-slide rack and fixed with 4% vol./vol. phosphate-buffered formaldehyde for 20 minutes and washed with PBS (2x2 minutes). The sections were then incubated in DHE for 5 min before washing with PBS (2x2 minutes). DAPI solution (300nM) were applied to all sections and incubated in the dark for 3 minutes before washing with PBS (2x2 minutes). All sections were air-dried before mounting with ProLong Gold Antifade Reagent and covered with a glass cover. Photos of the sections were then taken in Apotome Axioplan 2 Imaging Microscope at 20x magnification.

#### *4.5.2.3 Gr1(Ly6C) and DAPI*

The inflammation response caused by lipid accumulation in the arterial wall during atherosclerosis causes monocytes and lymphocytes to be recruited to the site of the lesion [17, 52], one such monocyte are the Gr1(Ly6C) macrophages. Mice have mainly two subsets, $Gr1(Ly6C)^{lo}$ and $Gr1(Ly6C)^{hi}$, were the latter is involved in the inflammatory response [53].
Gr1(Ly6C)-antigen specific antibodies can be used to detect the presence of inflammation in tissue sections. If any inflammation is present in the sample, it can be detected by studying the amount of Gr1(Ly6C) present after optical microscopy.

#### 4.5.2.3.1 Aortic root

Glass slides with frozen sections of aortic roots from one level were thawed and placed in a 24-slide rack. All steps were carried out in room temperature.

The slides were then blocked in 1% BSA/PBS for 1 hour and then washed 2 times in PBS for 2 minutes each. The sections were then fixated in 4% vol./vol. phosphate-buffered formaldehyde for 5 minutes and then washed (2x2 minutes) in PBS. A thin line of paraffin wax was then drawn around all sections on the slides to prevent leakage. Gr1(Ly6C) antibody (1:500), mixed in PBS containing 0.1% BSA, was then applied to the slides and incubated for 1 hour in the dark. All solution was poured off and all slides were washed in PBS (2x2 minutes). The secondary antibody solution was made by adding anti-rat Alexa 594 in 1% BSA/PBS (1:1000), added to all sections and left for incubation for 1.5 hour under cover. All slides were washed with PBS (2x2 minutes) and DAPI solution (300nM) was applied to all sections and incubated for 3 minutes under cover. All slides were washed with PBS (2x2 minutes) and air-dried before mounting with ProLong Gold Antifade Reagent and covered with a glass cover. Photos of the sections were then taken in Apotome Axioplan 2 Imaging Microscope at 20x magnification.

#### 4.5.2.3.2 Liver sections

Glass slides with liver sections fixed in paraffin (sectioning done by Histocenter, Gothenburg, Sweden) were placed in a 24-slide rack and deparaffinised by immersing the sections in xylene/ xylene/ ethanol (96%)/ ethanol (96%)/ ethanol (75%) / ethanol (50%) for 10/5/5/5/5/5 minutes, respectively. All slides were then washed one time in PBS before being removed from the rack. A thin line of paraffin wax was then drawn around all sections on the slides to prevent leakage. Gr1(Ly6C) antibody (1:500) mixed in PBS-T containing 0.1% BSA was then applied to the slides and incubated for 1.5 hour in the dark. All solution was then poured off and all slides were washed in PBS (2x2 minutes). The secondary antibody solution was mixed by adding anti-rat Alexa 594 in 1% BSA/PBS (1:1000) and added to all sections and left for incubation for 2 hours under cover. All slides were washed with PBS (2x2 minutes) and DAPI solution (300nM) were applied to all sections and incubated for 3 minutes. All slides were washed with PBS (2x2 minutes) and air-dried before mounting with ProLong Gold Antifade Reagent and covered with a glass cover. Photos of the sections were then taken in Apotome Axioplan 2 Imaging Microscope at 20x and 40x magnification.

## 4.6 Image analysis and quantification

For aortic roots stained with ORO, the area of all plaques in the sections were measured by using the ImageJ software. For all other stainings, the area stained was quantified in 5 randomly selected microscopic fields. Signals were quantified by using the ImageJ software, with set parameters for detection. The same parameters were used for all pictures from each procedure. The percentage of signal area was calculated from the total area.

## 4.7 Statistical calculations

Statistical significance between two groups was evaluated using the unpaired two-tailed Student's *t* test and among more than two groups by analysis of one-way ANOVA followed by *t* test for post-hoc analysis. Differences were considered statistically significant at a *P* value $< 0.05$. All statistical analyses were performed using SPSS Statistics.

# 5 Results

## 5.1 Confirmation of mice model

One injection of rAAV hPCSK9 was sufficient to significantly increase the relative mRNA expression of hPCSK9 in both the liver from the KO and TG cohort, and their saline injected WT control groups (Figure 4A-B). Correspondingly, a significant decrease of the hepatic LDLR protein levels was seen in all hPCSK9-injected mice (Figure 4C-D), which further confirms that the hPCSK9 indeed causes increased degradation of the LDLR.

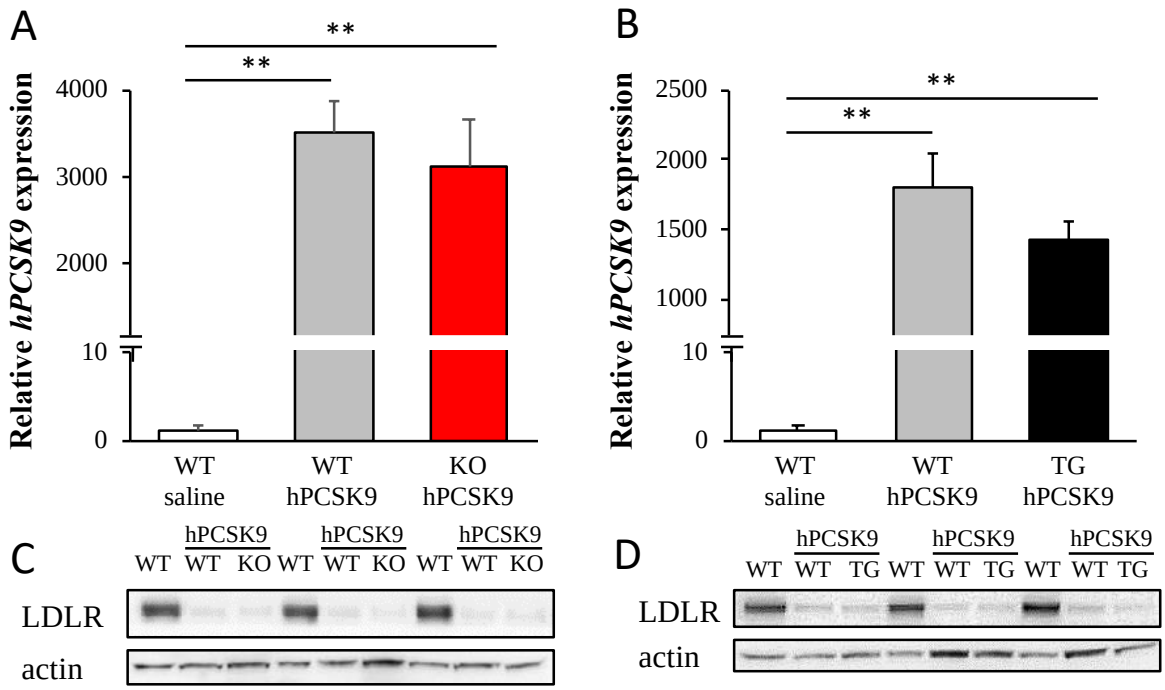


**Figure 4: Relative hepatic mRNA expression of hPCSK9 assessed by qRT-PCR for A) KO cohort B) TG cohort and Western blot analysis of liver lysate with LDLR-specific antibodies and actin control for C) KO cohort D) TG cohort. The mRNA expression level in saline-injected wild-type mice is set to 1. Representative Western blots are shown with actin used as a loading control. ** P<0.01**

## 5.2 Aortic root studies

### 5.2.1 STK25 staining – Expression in the cardiovascular system

The expression of STK25 in various tissues, such as liver, skeletal muscle and adipose tissue has been extensively studied [9, 10, 54, 55], but the expression of STK25 in the cardiovascular system is not known. *Stk25* antibody was used together with DAPI to visualize the localization and distribution of STK25 in aortic root sections (Figure 5, enlarged pictures in Appendix A2).

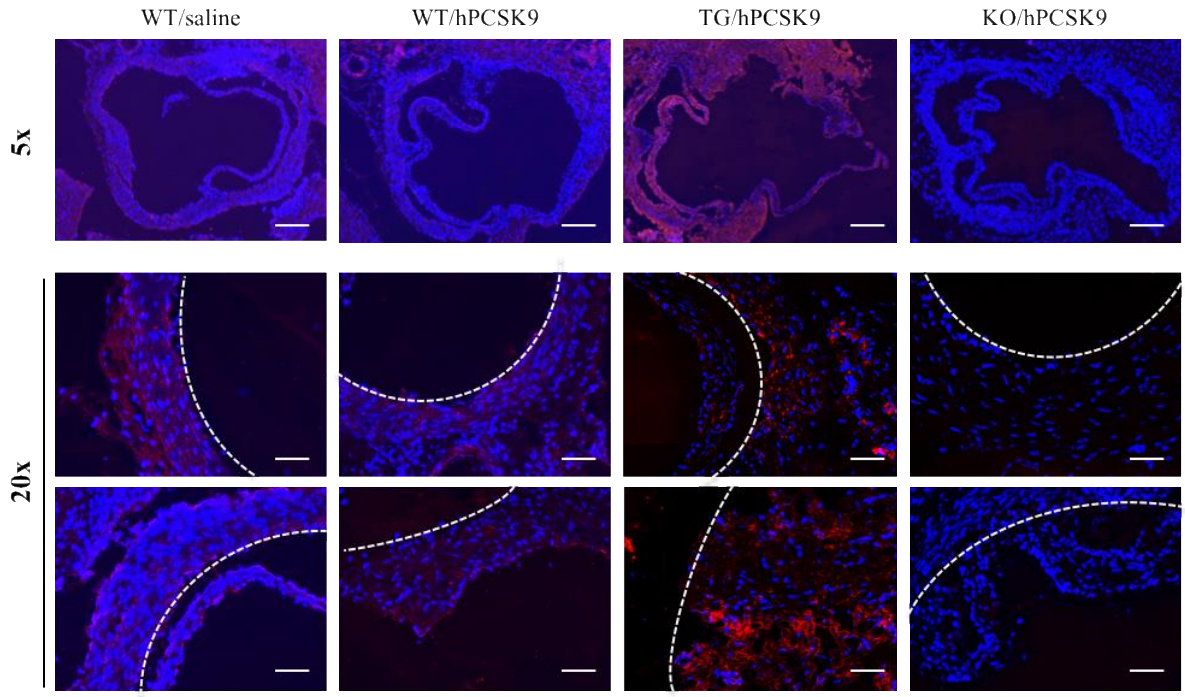


**Figure 5: Representative immunofluorescence analysis of aortic root sections with STK25 antibodies (red) and nucleus staining by DAPI (blue) at 5x and 20x magnification. Dotted line separates arterial wall from lumen. Scale bar 200 µm at 5x and 50 µm at 20x.**

Expression of STK25 (seen in red in Figure 5) can be seen evenly distributed throughout the aortic wall for the WT/saline, WT/hPCSK9 and for TG/hPCSK9 mice, but no protein was detected in the KO/hPCSK9 mice.

The expression of *Stk25* in both saline and hPCSK9-injected groups confirms that the injections do not affect the expression pattern of the protein.

### 5.2.2 ORO staining – Difference in fat accumulation in aortic root

The hypothesis that STK25 can affect the progress of CVDs, and in particular atherosclerosis, was studied and evaluated by ORO stained sections of the aortic root from hPCSK9-treated KO and TG mice and their corresponding hPCSK9-injected WT littermates.

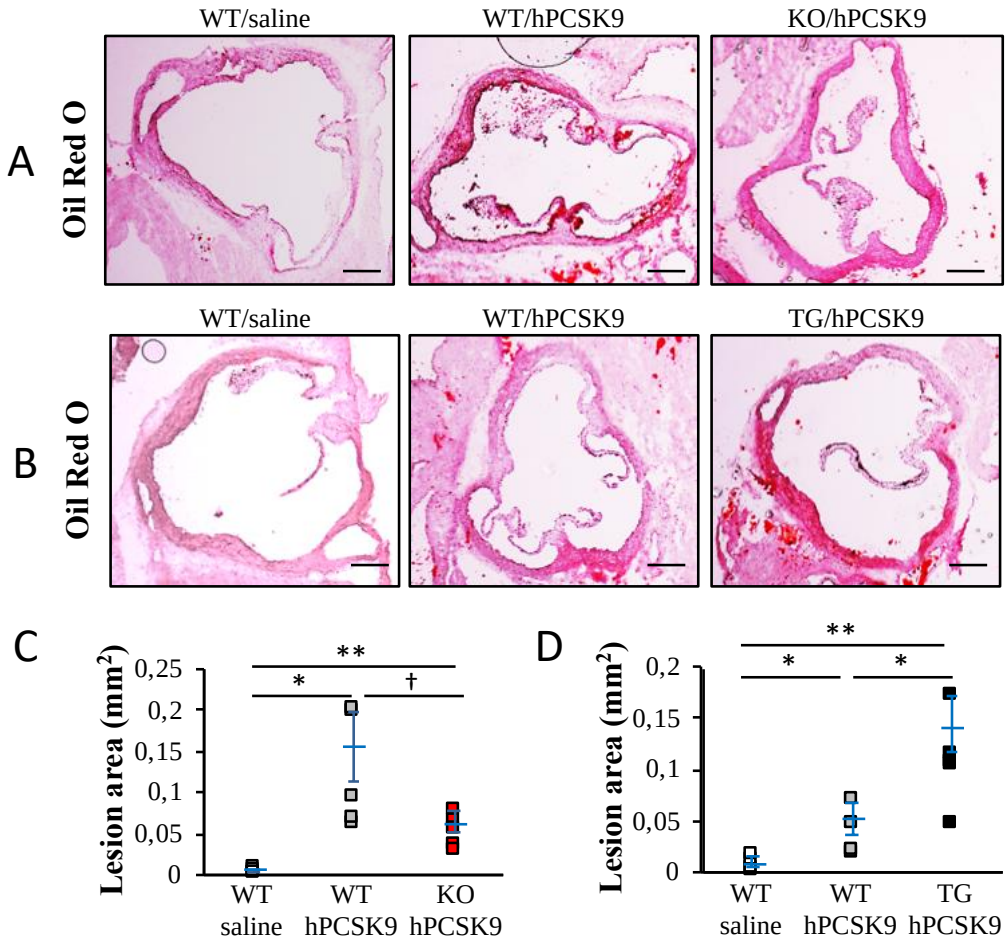


**Figure 6: Representative pictures of Oil Red O stained aortic root sections from A) KO cohort B) TG cohort together with corresponding lesion area (C-D). Lipid accumulation in red colour. Scale bar 200 µm. Data are mean ± SEM. KO) n=4-10 mice per group TG) n=4-8 mice per group. †<0.1 * P<0.05 ** P<0.01**

The typical feature of atherosclerosis is an accumulation of lipids and fatty lesions in the wall of the blood vessel, which can be observed in the ORO stained sections of the aortic root (Figure 6A-B) where the plaques can be seen in red. Increased plaque formation can be observed in the TG/hPSCK9 mice (Figure 6B and D), compared their corresponding WT/hPCSK9 (0.11 ± 0.02 vs. 0.04 ± 0.01 $mm^2$), suggesting that STK25 is involved in the progression of atherosclerosis. Further confirmation is provided by the reduction of lesion area found in the KO/hPSCK9 mice (Figure 6C). Example of other Oil Red O aortic root sections can be found in Appendix A1.

### 5.2.3 Picrosirius Red – Plaque progression

A single injection of rAAV hPCSK9 was sufficient to cause western-type diet fed mice to form lesions. The plaque progression was studied by staining of aortic root sections with Picrosirus Red, where an increase of fibrosis in the plaque in the aortic root was seen in hPCSK9-injected mice compared to the WT/saline groups (Figure 7A-B).

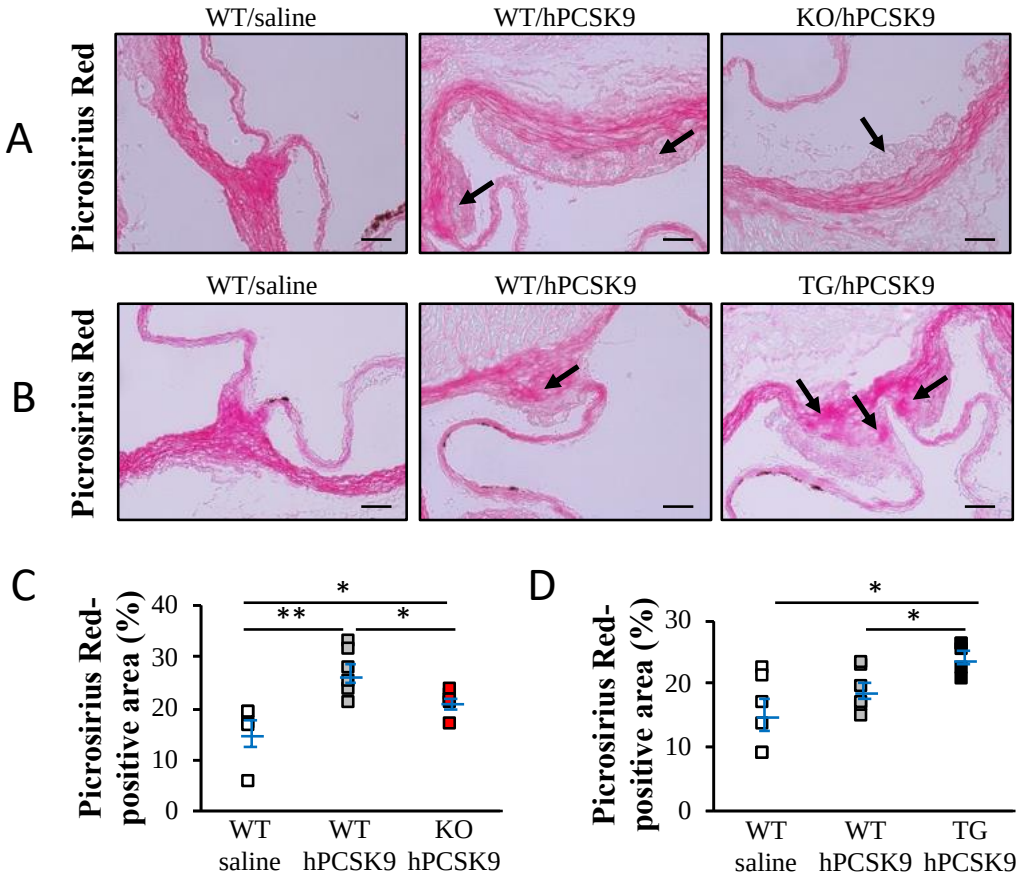


**Figure 7: Representative pictures of Picrosirius Red stained cusps of aortic root sections A) KO cohorts B) TG cohort and quantitative analysis of plaque formation C) KO cohort D) TG cohort. Arrow indicate fibrous content. Scale bar 40 µm. Data are mean ± SEM. KO) n=6-10 mice per group TG) n= 5-10 mice per group. * P<0.05 ** P<0.01**

The quantitative analysis of the Picrosirius Red stained sections was consistent with the results seen in the ORO stained aortic root section. A higher amount of aggravated fibrous plaque was seen in the TG/hPCSK9 mice compared to their WT/hPCSK9 littermates, while the KO/hPCSK9 mice had significantly lower levels of fibrosis compared to their WT/hPCSK9 controls (Figure 7C and D). These results show that STK25 have an impact on the plaque progression. Of note, significant increase in lesions was seen in all groups of mice injected with hPCSK9 compared with saline-treated controls showing that the hPCSK9-injections had the expected effect.

### 5.2.4 Gr1(Ly6C) – Inflammatory infiltration

Inflammation and swelling are common occurrence during atherosclerosis progression. Sections of the aortic root were incubated with Gr1(Ly6C) antibodies to find signs of inflammation (Figure 8A-B).

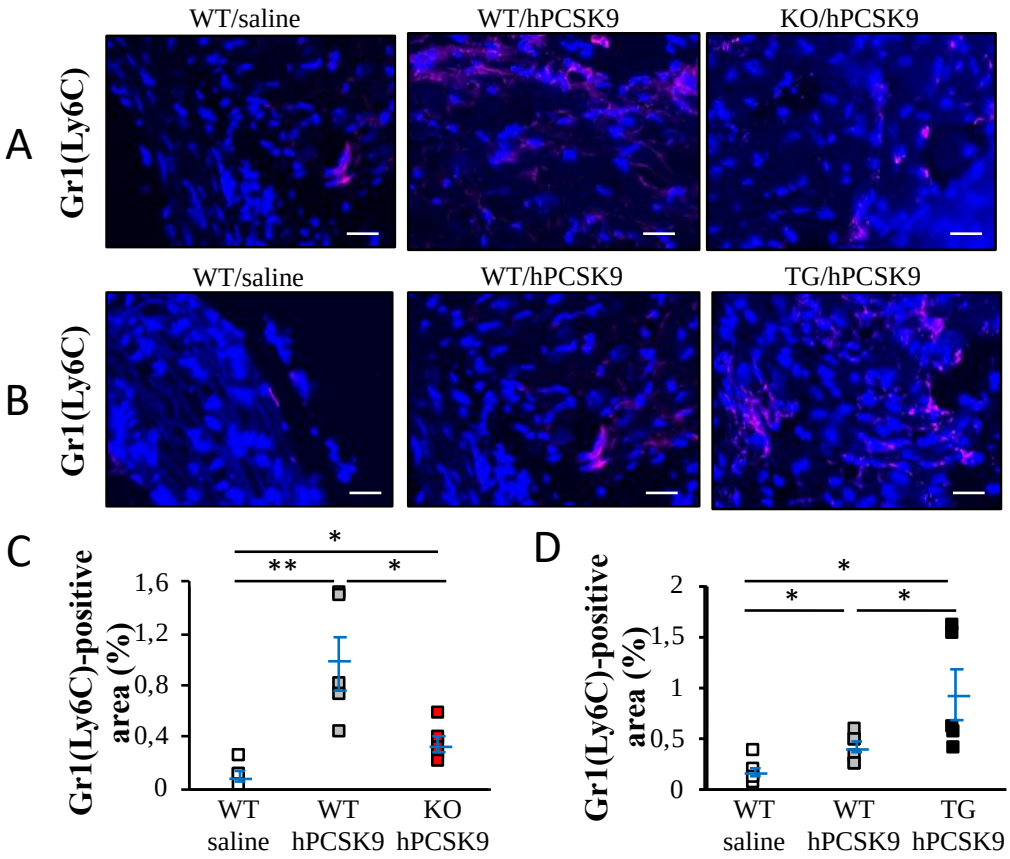


**Figure 8: Representative pictures of Gr1(Ly6C) in aortic root section visualized by immunofluorescences for A) KO cohort B) TG cohort. DAPI in blue and Gr1(Ly6C) in pink. Quantitative analysis of positive signal area for C) KO cohort D) TG cohort. Scale bar 40 µm. Data are mean ± SEM. KO) n=4-10 mice per group TG) n=4-8 mice per group. * P<0.05 ** P<0.01.**

The levels of positive signal for the TG/hPCSK9 mice were significantly increased compared to WT/hPCSK9 (Figure 8D), while less inflammation could be observed in the KO/hPCSK9 mice (Figure 8C), when compared to their WT/hPCSK9 littermates. Low levels of inflammation could be seen in the WT/saline group for both cohorts, confirming again that the hPSCK9 injections had the expected effect on atherosclerosis development.

### 5.2.5 DHE – Oxidative stress response

Oxidative stress is a common factor in atherosclerosis. Several steps during the progression of the plaque formation cause ROS to be released into the surrounding tissues. ROS has also been found to be part of the oxidation process of LDL that causes lipid accumulation in the subendothelial layer of the blood vessels. The oxidative stress response in the cardiovascular system in hPCSK9-injected western-type diet fed mice was therefore studied by staining aortic root sections with DHE (Figure 9A-B).

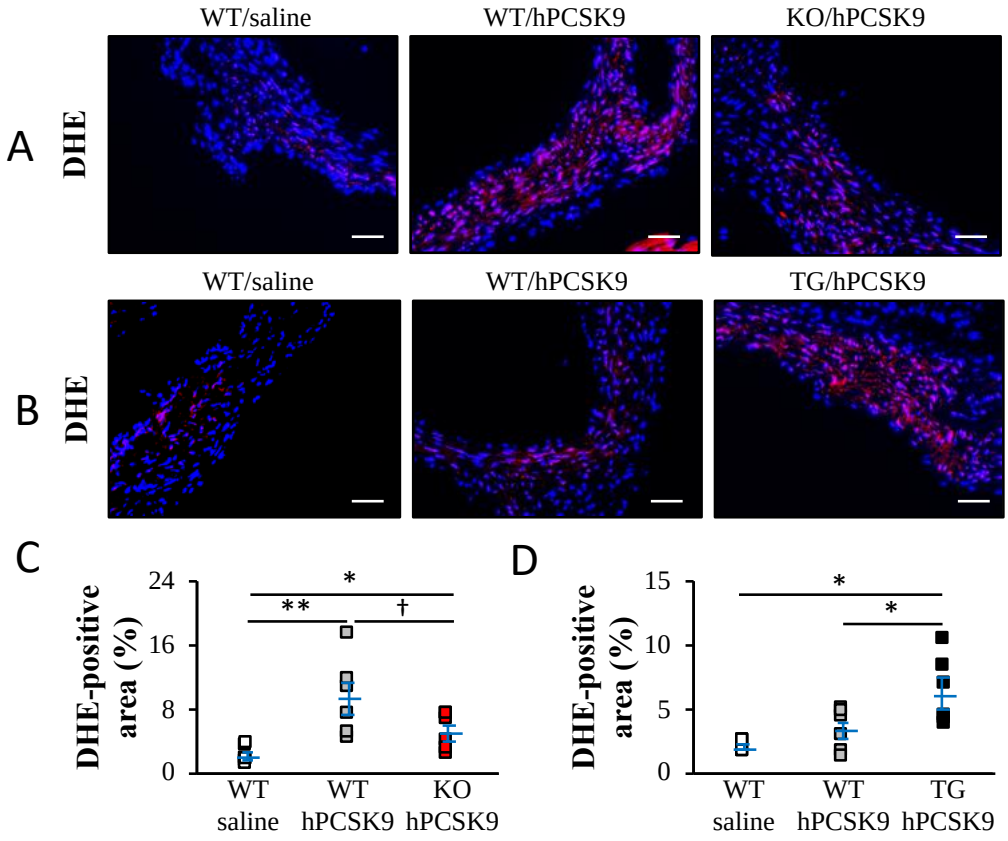


**Figure 9: Representative pictures of DHE stained aortic sinuses from A) KO cohort B) TG cohort. DAPI seen in blue and DHE seen in red. Quantitative analysis of DHE positive signal from C) KO cohort D) TG cohort. Scale bar 40 µm. Data are mean ± SEM. KO) n=4-10 mice per group TG) n=4-8 mice per group. †<0.1 * P<0.05 ** P<0.01.**

A clear increase of oxidative stress was seen in the TG/hPCSK9 mice, while a reduction was seen in the KO/hPCSK9 mice, compared to their corresponding WT/hPCSK9 littermates (Figure 9C-D). These results are consistent with earlier result, with a higher plaque formation and increased inflammatory infiltration, further indicating that STK25 is an important regulator during the development of atherosclerosis.

## 5.3 Liver studies

### 5.3.1 Gr1(Ly6C) – Signs of inflammation in liver

A high inflammatory response is a sign of NASH. Signs of inflammation in the liver from the hPCSK9-injected mice were studied using Gr1(Ly6C) antibody.

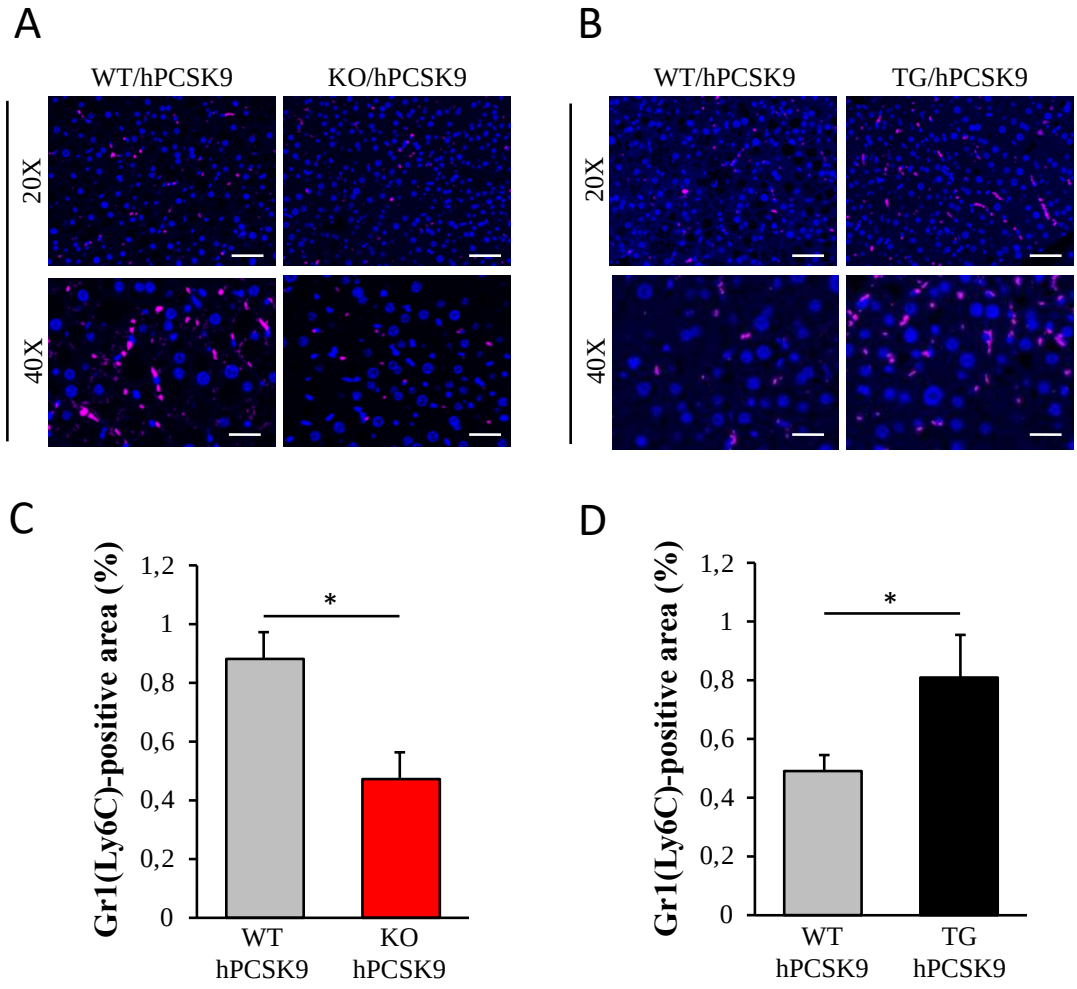


**Figure 10: Representative pictures of Gr1(Ly6C) in liver section visualized by immunofluorescenes for A) KO cohort B) TG cohort. DAPI in blue and Gr1(Ly6C) in pink. Quantitative analysis of positive signal area for C) KO cohort D) TG cohort. Scale bar 50 µm at 20x and 25 µm at 40x. Data are mean ± SEM. KO) n=6-10 mice per group TG) n=5-8 mice per group. * P<0.05.**

A significant increase in Gr1(Ly6C) positive signal was found in the liver sections from the TG/hPCSK9 mice, while the KO/hPCSK9 mice display decreased levels, compared to their corresponding WT/hPCSK9 controls (Figure 10A-D).

### 5.3.2 Hydroxyproline – NAFLD/NASH development

To further confirm that the NAFLD/NASH progression was affected in the mouse model used, the hydroxyproline content in liver lysate was measured. The effect of STK25 in NAFLD and NASH progression have previously been shown in high-fat diet and methionine and choline-deficient diet fed mice [3, 8], where *Stk25* TG mice displayed a higher prevalence for developing NASH compared to their WT littermates, while the reciprocal effect was seen in *Stk25* KO mice.

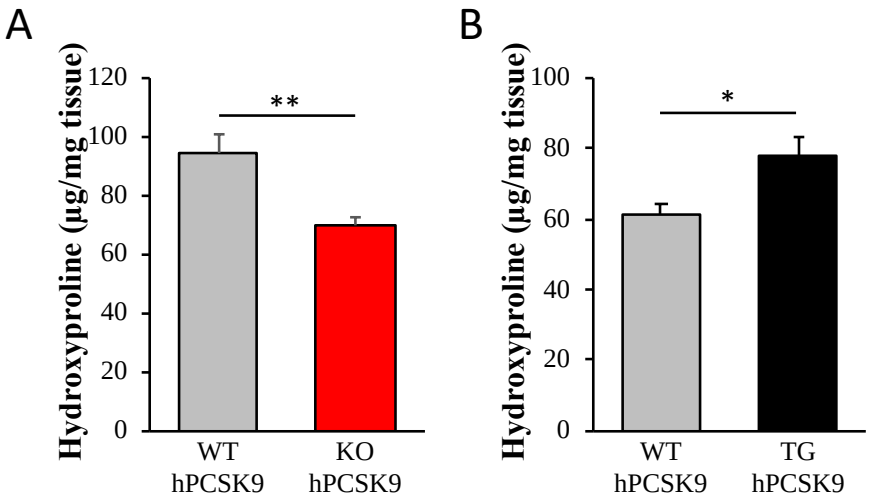


**Figure 11: Hydroxyproline content in liver lysate from A) KO cohort B) TG cohort. Data are mean ± SEM. KO) n=6-10 mice per group TG) n=5-8 mice per group. * P<0.05 ** P<0.01.**

High levels of hydroxyproline is a sign of fibrosis and of NASH progression. A significant reduction in hydroxyproline levels was observed in KO/hPCSK9 mice compared to the WT/hPCSK9 mice, and an increase in the levels was seen in the TG/hPCSK9 mice compared to their WT/hPCSK9 (Figure 11A-B).

### 5.3.3 AST – Sign of damage in the liver

Increased levels of AST in blood samples is a sign of an immune system-mediated response from the liver cells. The AST activity in plasma samples from the rAAV8 was therefore measured to ensure that the viral vector did not cause any hepatotoxicity.

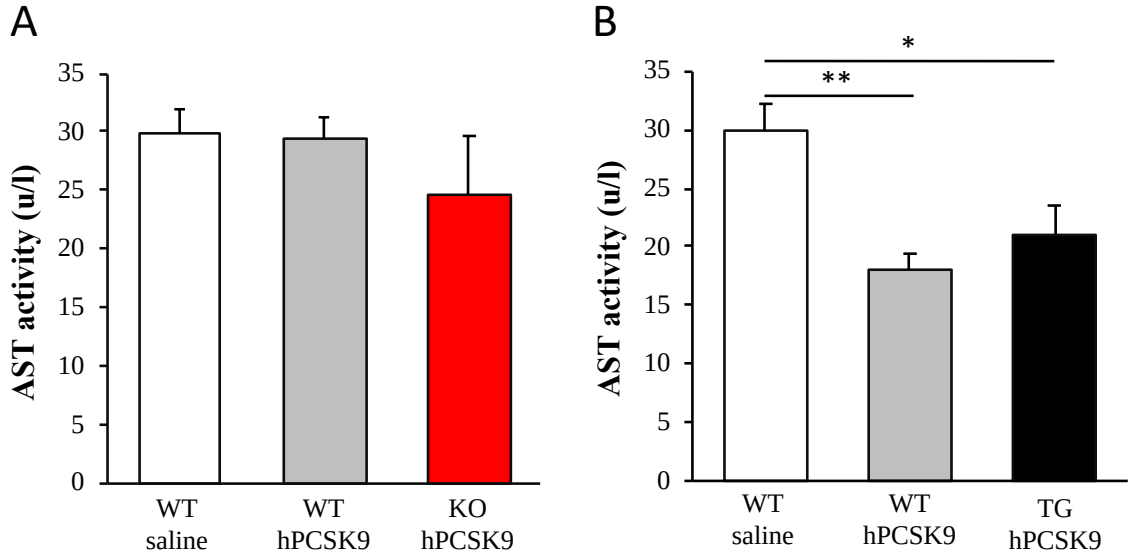


**Figure 12: AST activity from plasma samples from A) KO cohort B) TG cohort. Data are mean ± SEM. KO) n=5-10 mice per group TG) n=7-8 mice per group. * P<0.05 ** P<0.01.**

No significant changes in the enzymatic activity could be observed in the KO cohort, while a decrease in AST activity was observed in the TG cohort (Figure 12A-B). This provides evidence that the rAAV viral infection did not cause any adverse responses in the liver, since the hPCSK9-injected mice show no increase in the activity of AST post-injection when compared to the WT/saline group.

# 6 Discussion

The results from this project provide convincing evidence that STK25 is atherogenic and that the kinase is an important regulator in the progression of atherosclerosis. This provides good possibilities to reduce the risk of CVDs, but also to develop possible treatments, since many positive effects from the knockdown of STK25 could be observed. The KO/hPCSK9 mice showed less arterial lipid accumulation, aggravated plaque formation and signs of cell damage, such as oxidative stress and inflammatory response. Reciprocally, the TG/hPCSK9 mice displayed increased lesion area, increased severity of the plaques, with collagen rich cores, and more signs of cell damage, all signs of increased atherosclerosis.

The status of the liver in the KO mice was also improved since less signs of hepatic fibrosis and inflammation could be detected, while the TG mice had more signs of liver fibrosis and hepatocyte damage, proven by the hydroxyproline levels and the presence of Gr1(Ly6C) macrophages, which are signs of NASH.

The results from this project also confirms that a single injection of rAAV hPCSK9 is enough to induce and cause atherosclerosis in mice. The preferred model for atherosclerosis has been to use apolipoprotein E-deficient or LDLR-deficient mice [56], but the use of rAAV hPCSK9-induced LDLR-reduction in mice provides the same result without any time loss for crossbreeding. The method is also more economical since the cost will be reduced due to less animals and materials being used, and the ethical qualities will be improved as well. This is in line with the increasing environmental awareness today, which demands a reduction in resources being used by the industry, and that less animal is used, in compliance with the 3R principle (replacement, reduction and refinement) for animal research [57].

The fact that the use of a hepatocyte specific rAAV viral infection did not affect the function of the liver, is a positive result. The AST activity in KO/hPCSK9 mice was not changed, while the TG/hPCSK9 mice displayed a decrease in the activity post-injection compared to their corresponding WT/saline. These results show that the viral vector used does not cause any immune response in the hepatocytes.

STK25 can be observed in all parts of the aortic root (Figure 5). No positive signal was detected in the KO/hPCSK9 mice, which is expected, while an increase can be seen in the TG/hPCSK9 mice, which confirms the specificity of the antibody. The expression of the kinase is evenly distributed throughout the different layers and no accumulation in any specific cell types was seen. This provides the possibility that the increased presence and development of atherosclerosis in the TG/hPCSK9 mice is due to the influence of STK25 directly, and not through the effects of STK25 in liver.

The possibility of STK25 as a mediator in the complex and integrated molecular network underlying association between NAFLD/NASH and CVDs can not be concluded from this project alone, even though there are signs of both improved NASH and atherosclerosis in *Stk25* KO mice, while *Stk25* TG mice display a deterioration. More likely, STK25 have an independent effect in the aorta during the development of atherosclerosis, as well as an independent effect in the liver during NASH progression.

The risk of developing CVDs increases for people suffering from T2D, NAFLD/NASH and obesity. From this project, it can be confirmed that STK25 increases the possibility of developing atherosclerosis and that the kinase increases the progression of NASH present in

the liver. Earlier studies have confirmed that STK25 causes reduced glucose tolerance and insulin sensitivity [11], which are some of the first signs of T2D. The overexpression of STK25 in mice have also shown an increase in the presence of NASH [3, 8], while KO mice showed improved liver function and a lower tendency to develop NASH. Together with the findings in this study, showing a role of STK25 in atherosclerosis, this provides a good opportunity to develop STK25 inhibitors that targets more than one metabolic disease or disorder. The possibility to provide a treatment for several disorders at the same time would greatly benefit the society both economically, since less money is spent on treatments and healthcare, but also environmentally, since resources are being saved.

## 6.1 Outlook and further research

The number of overweight and obese people will only increase, together with the prevalence of related conditions such as CVDs and T2D, and the future demand on the society will be high. A possible treatment target for several of these metabolic diseases could be STK25, but in order for that to be a prospect, further studies are warranted.

It is not yet fully known by which mechanisms the kinase has its effects and what it regulates exactly, but the understanding about it is growing, which this project helped contribute to. It is known that STK25 plays an important role in metabolic regulation in liver, skeletal muscle and pancreas [3, 8, 9, 11, 25, 54, 55], and with this study also in the aorta, but there is still many other organs and tissues that can be affected. It would therefore be beneficial to further test the effects of STK25 in other tissues prone to metabolic damage.

In the regard of STK25 affecting the progression of CVDs, it would be interesting to evaluate the kinase expression in the heart and what other possible consequences STK25 might have there. It would also be interesting to test if STK25 causes any other symptoms present during atherosclerosis, such as hypertension or increased plaque ruptures, a risk factor of coronary infarction.

Future studies are needed to understand the upstream regulators, and the downstream targets, in the STK25 signalling pathway and a further continuation of the research of STK25 would be to find out how the kinase would be used as a treatment target.

# 7 Conclusions

The kinase STK25 has been found to be an important regulator in metabolic disorders, where it controls ectopic lipid storage, meta-inflammation and progression of NAFLD and NASH. The results from this study further suggest that STK25 also has a role in the development of atherosclerosis. Less aggravated plaque formation and less maturation could be found in *Stk25* KO/hPCSK9 mice, while *Stk25* TG/hPCSK9 mice displayed an increase in plaque formation, inflammation, fibrosis and oxidative stress response, as well as increased signs of liver damage. These results show a promising future to reach the goal to better understand the pathophysiological links between diet-induced conditions and CVDs, but also how to treat them. Continuing studies are needed to understand molecular mechanisms underlying the physiological effects of STK25.

# 8 References


[1] WHO | Obesity and overweight. *WHO*, http://www.who.int/mediacentre/factsheets/fs311/en/ (accessed 30 October 2017).

[2] Ballantyne CM, Hoogeveen RC, McNeill AM, et al. Metabolic Syndrome Risk for Cardiovascular Disease and Diabetes in the ARIC Study. *Int J Obes 2005* 2008; 32: S21–S24.

[3] Amrutkar M, Chursa U, Kern M, et al. STK25 is a critical determinant in nonalcoholic steatohepatitis. *FASEB J* 2016; 30: 3628–3643.

[4] Dave D, Doytch N, Kelly IR. Nutrient intake: A cross-national analysis of trends and economic correlates. *Soc Sci Med* 2016; 158: 158–167.

[5] WHO | Cardiovascular diseases (CVDs). *WHO*, http://www.who.int/mediacentre/factsheets/fs317/en/ (accessed 6 November 2017).

[6] Marchesini G, Bugianesi E, Forlani G, et al. Nonalcoholic fatty liver, steatohepatitis, and the metabolic syndrome. *Hepatology* 2003; 37: 917–923.

[7] Portillo-Sanchez P, Cusi K. Treatment of Nonalcoholic Fatty Liver Disease (NAFLD) in patients with Type 2 Diabetes Mellitus. *Clin Diabetes Endocrinol Lond*; 2. Epub ahead of print 2016. DOI: http://dx.doi.org.proxy.lib.chalmers.se/10.1186/s40842-016-0027-7.

[8] Amrutkar M, Cansby E, Nuñez-Durán E, et al. Protein kinase STK25 regulates hepatic lipid partitioning and progression of liver steatosis and NASH. *FASEB J* 2015; 29: 1564–1576.

[9] Amrutkar M, Cansby E, Chursa U, et al. Genetic Disruption of Protein Kinase STK25 Ameliorates Metabolic Defects in a Diet-Induced Type 2 Diabetes Model. *Diabetes* 2015; 64: 2791–2804.

[10] Nerstedt A, Cansby E, Andersson CX, et al. Serine/threonine protein kinase 25 (STK25): a novel negative regulator of lipid and glucose metabolism in rodent and human skeletal muscle. *Diabetologia* 2012; 55: 1797–1807.

[11] Cansby E, Amrutkar M, Holm LM, et al. Increased expression of STK25 leads to impaired glucose utilization and insulin sensitivity in mice challenged with a high-fat diet. *FASEB J* 2013; 27: 3660–3671.

[12] Bjørklund MM, Hollensen AK, Hagensen MK, et al. Induction of Atherosclerosis in Mice and Hamsters Without Germline Genetic EngineeringNovelty and Significance. *Circ Res* 2014; 114: 1684–1689.

[13] Grundy SM. Obesity, Metabolic Syndrome, and Cardiovascular Disease. *J Clin Endocrinol Metab* 2004; 89: 2595–2600.

[14] Bagchi D, Nair S. *Nutritional and Therapeutic Interventions for Diabetes and Metabolic Syndrome*. San Diego, UNITED STATES: Elsevier Science, http://ebookcentral.proquest.com/lib/chalmers/detail.action?docID=860151 (2012, accessed 22 January 2018).

[15] Huang PL. A comprehensive definition for metabolic syndrome. *Dis Model Mech* 2009; 2: 231–237.

[16] Ha KH, Kim DJ. Trends in the Impact of Diabetes on the Development of Cardiovascular Diseases. *Circ J* 2016; 80: 2293–2294.

[17] Lusis AJ. Atherosclerosis. *Nat Lond* 2000; 407: 233–41.

[18] Bentzon JF, Otsuka F, Virmani R, et al. Mechanisms of Plaque Formation and Rupture. *Circ Res* 2014; 114: 1852–1866.

[19] Wal VD, C A, Becker AE. Atherosclerotic plaque rupture – pathologic basis of plaque stability and instability. *Cardiovasc Res* 1999; 41: 334–344.

[20] Charitos EI, Sievers H-H. Anatomy of the aortic root: implications for valve-sparing surgery. *Ann Cardiothorac Surg* 2013; 2: 53–56.
[21] Loomba R, Sanyal AJ. The global NAFLD epidemic. *Nat Rev Gastroenterol Hepatol Lond* 2013; 10: 686–690.
[22] Michelotti GA, Machado MV, Diehl AM. NAFLD, NASH and liver cancer. *Nat Rev Gastroenterol Hepatol Lond* 2013; 10: 656–665.
[23] Neuschwander-Tetri BA. Future Treatments of NASH. *Curr Hepatol Rep* 2016; 15: 125–133.
[24] Pombo CM, Bonventre JV, Molnar A, et al. Activation of a human Ste20-like kinase by oxidant stress defines a novel stress response pathway. *EMBO J* 1996; 15: 4537–4546.
[25] Nuñez-Durán E, Aghajan M, Amrutkar M, et al. STK25 antisense oligonucleotide treatment reverses glucose intolerance, insulin resistance and nonalcoholic fatty liver disease in mice. *Press Hepatol Commun*.
[26] Lambert G, Sjouke B, Choque B, et al. The PCSK9 decade. *J Lipid Res* 2012; 53: 2515–2524.
[27] Kulseth MA, Berge KE, Bogsrud MP, et al. Analysis of LDLR mRNA in patients with familial hypercholesterolemia revealed a novel mutation in intron 14, which activates a cryptic splice site. *J Hum Genet* 2010; 55: 676.
[28] Mollaki V, Drogari E. Genetic causes of monogenic familial hypercholesterolemia in the Greek population: Lessons, mistakes, and the way forward. *J Clin Lipidol* 2016; 10: 748–756.
[29] Aschauer DF, Kreuz S, Rumpel S. Analysis of Transduction Efficiency, Tropism and Axonal Transport of AAV Serotypes 1, 2, 5, 6, 8 and 9 in the Mouse Brain. *PLoS One San Franc* 2013; 8: e76310.
[30] Ai J, Li J, Gessler DJ, et al. Adeno-associated virus serotype rh.10 displays strong muscle tropism following intraperitoneal delivery. *Sci Rep Nat Publ Group Lond* 2017; 7: 40336.
[31] Ldlr low density lipoprotein receptor [Mus musculus (house mouse)] - Gene - NCBI, https://www.ncbi.nlm.nih.gov/gene/16835 (accessed 27 January 2018).
[32] Addgene: Adeno-associated virus (AAV) Guide, https://www.addgene.org/viral-vectors/aav/aav-guide/ (accessed 15 January 2018).
[33] 000664 - C57BL/6J, https://www.jax.org/strain/000664 (accessed 24 January 2018).
[34] Fontaine DA, Davis DB. Attention to Background Strain Is Essential for Metabolic Research: C57BL/6 and the International Knockout Mouse Consortium. *Diabetes* 2016; 65: 25–33.
[35] Alturkistani HA, Tashkandi FM, Mohammedsaleh ZM. Histological Stains: A Literature Review and Case Study. *Glob J Health Sci* 2016; 8: 72–79.
[36] El-Bahrawy M, Ganesan R. Frozen section in gynaecology: uses and limitations. *Arch Gynecol Obstet* 2014; 289: 1165–1170.
[37] Farkas AE, Gerner-Smidt C, Lili L, et al. Cryosectioning Method for Microdissection of Murine Colonic Mucosa. *J Vis Exp JoVE*. Epub ahead of print 12 July 2015. DOI: 10.3791/53112.
[38] Histological Sample Prep for a Light Microscope | Protocol, https://www-jove-com.proxy.lib.chalmers.se/science-education/5039/histological-sample-preparation-for-light-microscopy (accessed 25 January 2018).
[39] Can You Stand the Cold? Cryosectioning for Beginners. *Bitesize Bio*, https://bitesizebio.com/28466/can-stand-cold-cryosectioning-beginners/ (2017, accessed 25 January 2018).

[40] Odell ID, Cook D. Immunofluorescence Techniques. *J Investig Dermatol Lond* 2013; 133: e4.
[41] Matsuki T, Chen J, Howell BW. Acute inactivation of the serine-threonine kinase Stk25 disrupts neuronal migration. *Neural Develop* 2013; 8: 21.
[42] Gabr SA, Alghadir AH. Prediction of fibrosis in hepatitis C patients: assessment using hydroxyproline and oxidative stress biomarkers. *VirusDisease* 2014; 25: 91–100.
[43] Trautwein C, Friedman SL, Schuppan D, et al. Hepatic fibrosis: Concept to treatment. *J Hepatol* 2015; 62: S15–S24.
[44] Mehlem A, Hagberg CE, Muhl L, et al. Imaging of neutral lipids by oil red O for analyzing the metabolic status in health and disease. *Nat Protoc* 2013; 8: 1149.
[45] Lattouf R, Younes R, Lutomski D, et al. Picrosirius Red Staining: A Useful Tool to Appraise Collagen Networks in Normal and Pathological Tissues. *J Histochem Cytochem* 2014; 62: 751–758.
[46] Segnani C, Ippolito C, Antonioli L, et al. Histochemical Detection of Collagen Fibers by Sirius Red/Fast Green Is More Sensitive than van Gieson or Sirius Red Alone in Normal and Inflamed Rat Colon. *PLoS ONE*; 10. Epub ahead of print 16 December 2015. DOI: 10.1371/journal.pone.0144630.
[47] Street JM, Souza ACP, Alvarez-Prats A, et al. Automated quantification of renal fibrosis with Sirius Red and polarization contrast microscopy. *Physiol Rep*; 2. Epub ahead of print 22 July 2014. DOI: 10.14814/phy2.12088.
[48] Okazaki I, Noro T, Tsutsui N, et al. Fibrogenesis and Carcinogenesis in Nonalcoholic Steatohepatitis (NASH): Involvement of Matrix Metalloproteinases (MMPs) and Tissue Inhibitors of Metalloproteinase (TIMPs). *Cancers* 2014; 6: 1220–1255.
[49] Lee R, Margaritis M, Channon K, et al. Evaluating Oxidative Stress in Human Cardiovascular Disease: Methodological Aspects and Considerations. *Curr Med Chem* 2012; 19: 2504–2520.
[50] DAPI 10236276001. *Sigma-Aldrich*, https://www.sigmaaldrich.com/catalog/product/roche/10236276001 (accessed 16 January 2018).
[51] Kapuscinski J. DAPI: a DNA-specific fluorescent probe. *Biotech Histochem Off Publ Biol Stain Comm* 1995; 70: 220–233.
[52] Galkina E, Ley K. Immune and Inflammatory Mechanisms of Atherosclerosis. *Annu Rev Immunol* 2009; 27: 165–197.
[53] Li D, Liu Y, Zhang X, et al. Inhibition of soluble epoxide hydrolase alleviated atherosclerosis by reducing monocyte infiltration in Ldlr−/− mice. *J Mol Cell Cardiol* 2016; 98: 128–137.
[54] Chursa U, Nuñez-Durán E, Cansby E, et al. Overexpression of protein kinase STK25 in mice exacerbates ectopic lipid accumulation, mitochondrial dysfunction and insulin resistance in skeletal muscle. *Diabetologia* 2017; 60: 553–567.
[55] Amrutkar M, Kern M, Nuñez-Durán E, et al. Protein kinase STK25 controls lipid partitioning in hepatocytes and correlates with liver fat content in humans. *Diabetologia* 2016; 59: 341–353.
[56] Meir KS, Leitersdorf E. Atherosclerosis in the Apolipoprotein E–Deficient Mouse: A Decade of Progress. *Arterioscler Thromb Vasc Biol* 2004; 24: 1006–1014.
[57] Törnqvist E, Annas A, Granath B, et al. Strategic focus on 3R principles reveals major reductions in the use of animals in pharmaceutical toxicity testing. *PLoS ONE*; 9: e101638.

# 9 Appendix

## A1 – Example of Oil Red O stained aortic root sections

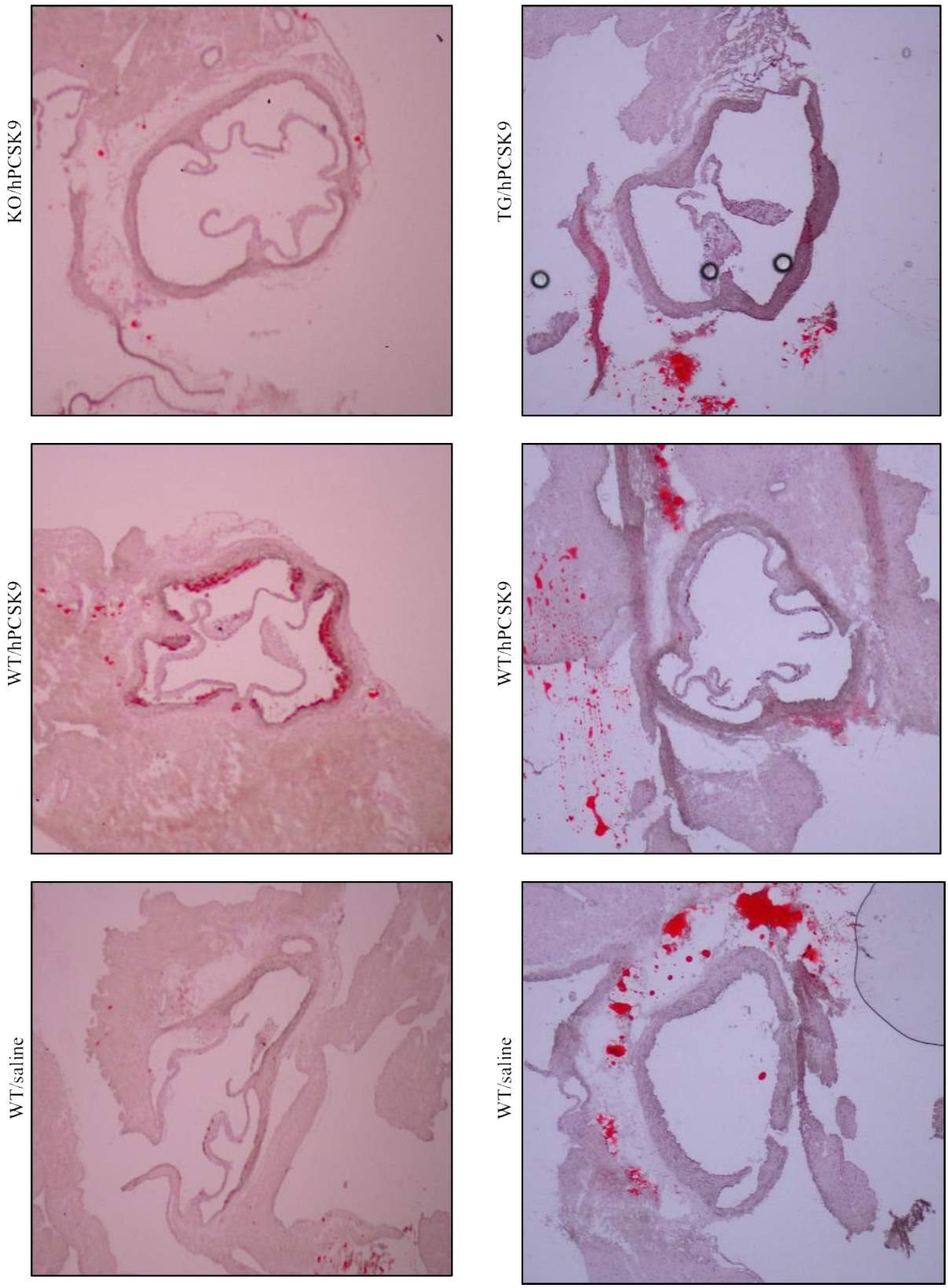

## A2 – Enlarged pictures of immunofluorescent detection of STK25